Structural Studies of Liquid-Crystalline Poly(ester amides)

N. S. Murthy* and S. M. Aharoni

Allied-Signal Inc., Research and Technology, Morristown, New Jersey 07962

Received July 2, 1991; Revised Manuscript Received October 28, 1991

ABSTRACT: The structure of a series of strictly alternating, hydrogen-bonded poly(ester amides) was studied by small- and wide-angle X-ray diffraction. These polymers have a generic structure $(-C(O)O(CH_2)_yOC(O)C_6H_4-NHC(O)(CH_2)_xC(O)NHC_6H_4-)_n$ and exhibit liquid-crystalline behavior in the melt when $y \geq 3$. Specimens quenched from the liquid-crystalline state have fluidlike disorder in the equatorial plane and long-range order along the chain axis and hence resemble the smectic phase. Diffuse and weak small-angle X-ray reflections with spacings longer than the chain-axis repeat are present when the polymer is in the quenched smectic phase, and they become sharp and intense as the crystalline order increases in the presence of a suitable plasticizer. The small-angle peaks are attributed to a lamellar structure in which ordered layers of hydrogen-bonded sheets are separated by less ordered domains. The hydrogen-bonded sheets within the lamellae are parallel to the fiber axis. The ester segments exist in more than one conformation and appear to be inclined at an angle of ~76° to the fiber axis. We speculate that the liquid-crystalline behavior observed by DSC and polarized light microscopy is due to the existence of hydrogen-bonded layers and lamellae. The series of small, postmelting transitions occur as the ester segments overcome the conformational barriers between the various rotational isomeric states. These transitions from one smectic liquid-crystalline phase to another could be a result of the variations in the stacking of the hydrogen-bonded layers in the lamellae.

Introduction

Polymers which exhibit liquid-crystalline (LC) behavior can be divided into two broad categories depending on whether the LC characteristics are due to the main chain or side groups. In many main-chain polymeric liquid crystals, the mesomorphic or LC phase is observed when the persistence length of the main chain is sufficiently large.[1] Flexible polymer chains can also exhibit LC behavior if they form macroscopic assemblies of asymmetric shapes.[2,3] A third class of liquid crystals is one in which clusters of ordered molecules are present in the molten state, i.e., after the melting of the three-dimensionally ordered crystals, because of the intermolecular hydrogen bonding.[4] An example of this last class of liquid crystals is the recently synthesized series of aromatic poly(ester amides) in which the aromatic amide segments are linked by ester groups.[5-9]

The synthesis, conformation, and properties of highly regular, alternating, semicrystalline, hydrogen-bonded (H-bonded) poly(ester amides) (PEA)

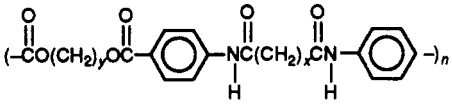

have been described earlier by Aharoni.[5] When $y = 2$, the transition from a semicrystalline solid to an isotropic melt occurs in a single step. But when $y \geq 3$ and $x > 4$, the melting of the crystalline solid into an isotropic fluid occurs in a series of steps which include a crystal–crystal transitions and a sequence of LC phases. These steps are first-order transitions. The number, temperature, and the enthalpy of these transitions depend on the length of the amide (y) and ester (x) segments.[5-7] In this report we present X-ray diffraction (XRD) results from polymers with y–x values of 3–3, 3–6, 3–7, 3–8, 3–14, and 5–14 and propose structural models for this family of polymers. The long spacing, which can be 3–6 times the repeat length of the monomer along the fiber axis, is attributed to the formation of lamellae consisting of layers of highly ordered H-bonded chains and the presence of disordered chains between these lamellae. We will discuss the effect of lamellar morphology and the H bonds on the various thermal transitions observed in these polymers.

Materials and Methods

The synthesis of these polymers has been described in an earlier publication.[5] Specimens of ~5-mil thickness were molded between aluminum foils and quenched in ice water. A set of samples were annealed for 15 min to 1 h at 100–200 °C in vacuum, and another set of samples were prepared by annealing in the presence of dimethylformamide (DMF) at 22–150 °C. A third series of films with $y = 3$ and $x = 3, 4, 7$, and 8 were oriented by drawing the cast films above their T_g. The 3–7 polymer dissolves in DMF even at room temperature, and therefore the swelling of 3–7 was controlled by adding methanol to DMF. Other polymers were heated either in the presence of DMF or after exposure to DMF. The 3–8 polymer was studied in most detail. Additional samples of the 3–8 polymer were prepared by quenching the molded specimen in DMF. A series of measurements from the 3–8 polymer were made under ambient conditions after immersing in DMF followed by exposure to temperatures from 22 to 200 °C.

Wide-angle X-ray diffraction (WAXD) and small-angle X-ray scattering (SAXS) measurements were carried out both at room temperature and at elevated temperatures. SAXS measurements at elevated temperatures were also carried out with the samples (3–8, 3–14, and 5–14) immersed in DMF in a quartz X-ray capillary; the 3–7 polymer, which is soluble in DMF, was studied in a mixture of DMF and methanol at room temperature.

WAXD scans were obtained on a Philips diffractometer in parafocus geometry. Variable-temperature WAXD scans were done using an Anton-Paar attachment. SAXS data were collected using a Tennelec one-dimensional position-sensitive detector mounted on a Franks camera.[10] The long spacings were calculated from the position of the peak maxima. Variable-temperature SAXS data were obtained by directing a stream of heated air at the desired temperature around the capillary containing the sample.

Solid-state carbon-13 NMR spectra were obtained using cross-polarization (CP) and magic-angle spinning (MAS) techniques[8,9] at 50.3 MHz on a Varian XL200 spectrometer equipped with Doty Scientific solid accessories. The magic angle was adjusted to within 0.1° using a ^{79}Br spectrum of KBr. The spectra were obtained with a 1-ms contact time and a 2-s repetition. Bloch decay (BD) spectra were also obtained from a film sample before and after exposure to DMF.

The differential scanning calorimeter (DSC) scans were obtained on a Du Pont DSC 9900 instrument. A total of 4–6

0024-9297/92/2225-1177$03.00/0

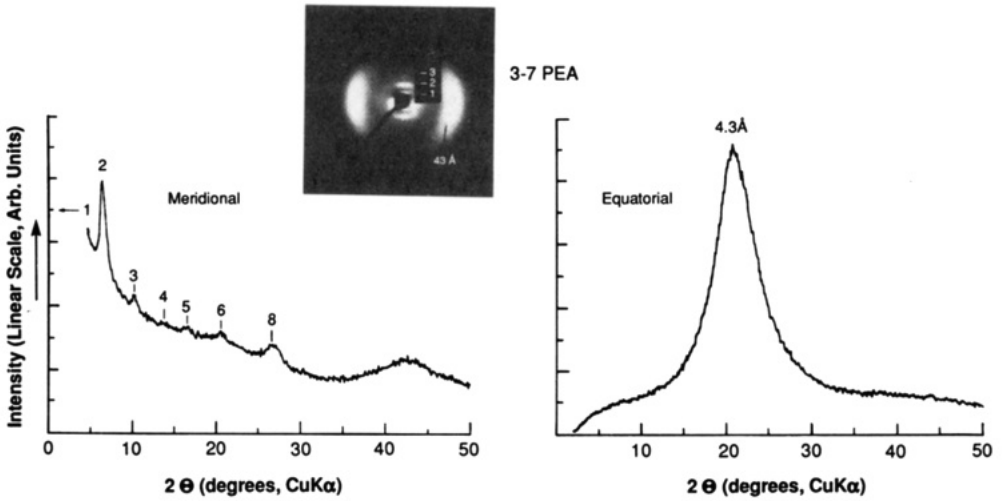

Figure 1. Representative XRD photograph and corresponding equatorial and meridional scans of 3–7 PEA.

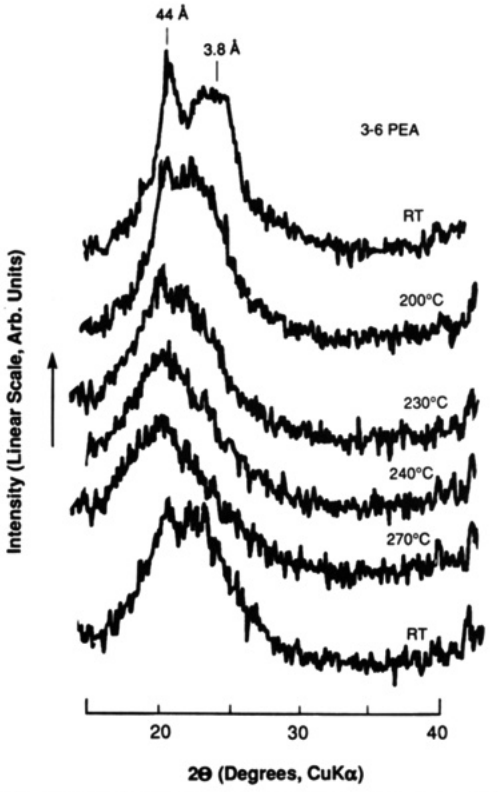

Figure 2. Variable-temperature WAXD scans from 3–6 PEA. The scans have been offset vertically.

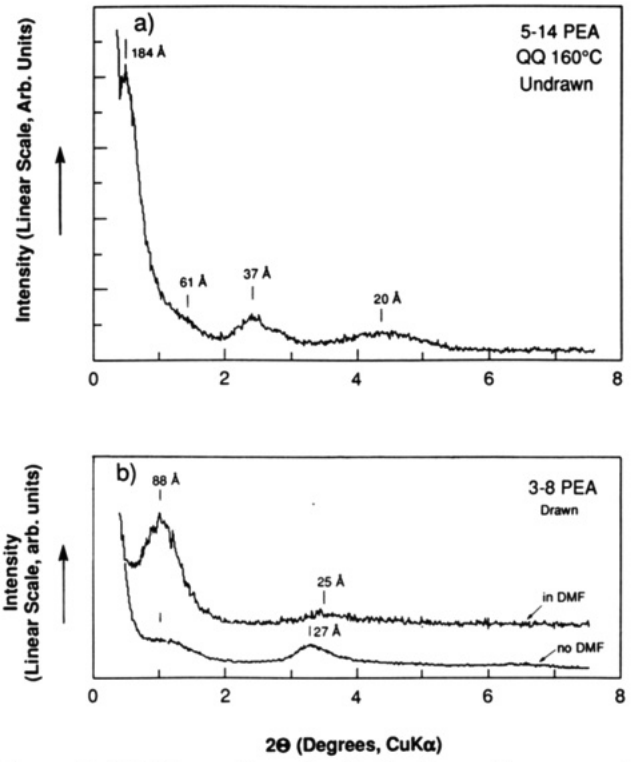

Figure 3. SAXS scans from (a) a 5–14 polymer film prepared by quenching in ice water from 160 °C and (b) a 3–8 polymer before and after exposure to DMF. The two 3–8 scans have been offset vertically.

mg of the material was sealed in a cell and heated at 10 °C/min.

Results

Figure 1 shows a diffraction photograph of an oriented 3–7 polymer along with the corresponding meridional and equatorial scans. This is typical of the data from PEAs in that all the polymers studied here show a diffuse equatorial halo and a series of sharp meridional reflections. In some polymers more than one fiber-axis repeat was observed. The wide-angle X-ray diffraction scans obtained at various temperatures (Figure 2) show that the polymer is essentially amorphous after the main melting endotherm, although the polarized microscope observations indicate the material to be LC.[5,6] The sample cooled from the melt is partially crystalline. Several specimens of the polymer, both semicrystalline samples and samples quenched from the LC phase, showed small-angle peaks with a repeat period (long spacing, L) ranging from 60 to 200 Å (Figures 3 and 4). Up to three reflections at 2θ = 2–6°, corresponding to d-spacings of 40–15 Å, were observed in many of the scans. These intermediate-angle peaks could not be indexed as higher order reflections of the lamellar spacing L.

The structural features which give rise to the SAXS peaks were investigated by studying PEA's swollen in DMF. SAXS data from 3–8 PEA films immersed in DMF are shown in Figure 3b. The small-angle peak becomes intense upon immersing the film in DMF, and, in many instances, the peak shifts to smaller angles. Both the d spacing and the intensity of the lamellar peak increase when the sample is heated in the presence of DMF. These changes occur rapidly within a few minutes. Note that the d spacings of the "higher order" reflections remain unchanged although the lamellar peak ($L > 50$ Å) shifts to smaller angles. Lamellar peaks with $L < 84$ Å were

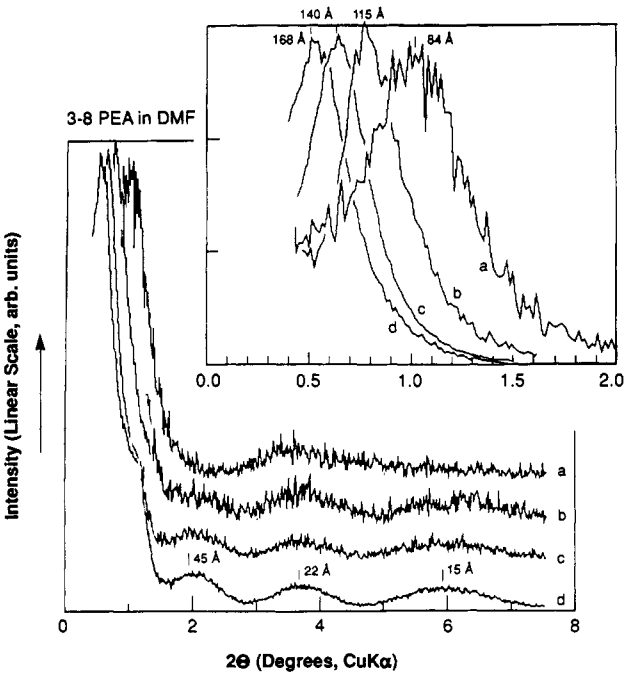

Figure 4. SAXS scans from drawn 3–8 samples in the dry state and in DMF at various temperatures. The intensity scale of the scans at $2\theta > 1.5°$ are enlarged by a factor of 1, 3, 7.5, and 8 times for scans a–d, respectively, and the scans have been offset vertically and scaled arbitrarily. The inset shows the data at $2\theta < 1.5°$.

Table I
SAXS Data from Oriented 3–7 PEA Films Swollen in Methanol/DMF[a]

volumetric ratio of methanol and DMF	L, Å	n
50:50	100	4
60:40	125	5
45:55	125	5
40:60	150	6

[a] L is the long spacing, and n is the number of monomer units in each lamella. The value of n and the chain-axis repeat, c, are calculated from the relation $L = nc$. The average value of c is 25 Å and is comparable to the WAXD value of 26.0 Å.

Table II
SAXS Data from Oriented 3–8 PEA Films[a]

sample history[b]	L,[c] Å	n[d]
in air at $T < 100$ °C or in DMF at $T < 50$ °C	86.1 (2.6)	3 (22)
in DMF at $T \sim 50$ °C or after annealing DMF-swollen film in air at $T < 175$ °C	112.8 (3.3)	4 (12)
DMF-swollen film annealed in air at $T \sim 175$ °C	137.3 (4.7)	5 (4)
same as above	166 (–)	6 (3)

[a] L is the long spacing, and n is the number of monomer units in each lamella. The value of n and the chain-axis repeat, c, are calculated from the relation $L = nc$. The average value of c is 28.4 Å, which is in good agreement with the WAXD value of 28.0 Å. [b] Unoriented films (molded at 250 °C) quenched in water (amorphous by WAXD) had no low-angle peaks. The same 250 °C molded films quick-quenched in DMF showed low-angle peaks of 84 Å when fresh and 110 and 135 Å upon aging. [c] Values in parentheses are standard deviations. [d] Values in parentheses are the number of observations.

frequently observed, but, unlike at $L > 84$ Å, the values at $L < 84$ Å were not reproducible. Exposure of 3–14 and 5–14 polymers to DMF at room temperature does not significantly change the SAXS. The SAXS data are summarized in Tables I–IV.

The effect of DMF on the WAXD pattern of PEA is illustrated in Figure 5 which shows the data from the 3–8

Table III
SAXS Data from Oriented 3–14 PEA Films[a]

sample history[b]	L,[c] Å	n[d]
oriented films either in ambient atmosphere or in DMF	67.5 (2.1)	2 (5)
unoriented film quick-quenched from 130 or 160 °C	102.3	3 (3)
unoriented film quick-quenched from 160 °C and aged 1.5 years, measured in air or in DMF at $T < 100$ °C	137 (–)	4 (4)
unoriented films quick-quenched from 160–225 °C; also oriented film aged for 1.5 years either in ambient atmosphere or in DMF	83.2 (2.5)	5_2 (7)

[a] L is the long spacing, and n is the number of monomer units in each lamella. The value of n and the chain-axis repeat, c, are calculated from the relation $L = nc$. The average value of c is 34.0 Å, which is same as the value from WAXD scans. [b] "Quick-quenched" samples were first molded into films at 250 °C and then slowly cooled to the indicated quench temperature. [c] Values in parentheses are standard deviations. [d] Values in parentheses are the number of observations. Subscript 2 in the last entry suggests that the observed peak is regarded as a second-order reflection.

Table IV
SAXS Data from Oriented 5–14 PEA Films[a]

sample history	L,[b] Å	n[d]
quenched from 255 °C	104	3 (1)
160 °C quenched film after slow cooling from 275 °C (film B) in DMF at $T < 100$ °C	140 (3.6)	4 (5)
film B in DMF at 100 °C < $T < 155$ °C; also observed in some B films at room temperature	60.3 (2.4)[c]	5_3 (18)
film B annealed in DMF at $T \sim 100$ °C; also observed in some unannealed B films	126 (2)	7_2 (4)

[a] L is the long spacing, and n is the number of monomer units in each lamella. The value of n and the chain-axis repeat, c, are calculated from the relation $L = nc$. The average value of c thus calculated is 35.5 Å and is in good agreement with the 35.6 Å value from WAXD scans. [b] The values in parentheses are standard deviations. [c] In one scan, a 180-Å spacing peak was barely noticeable. In many instances, however, the assignment of this peak as the third order of the ~180-Å spacings may be rather ambiguous because the ~60-Å spacings can also be regarded as the second order of the 120-Å reflection. [d] The numbers in parentheses are the number of observations. The subscripts refer to the assignments as the second- or third-order reflections.

polymer. The increase in the intensity of the crystalline peaks in the presence of DMF indicates an increase in the crystallinity of the polymer. This contributes to the increase in the intensity of the SAXS peak. There is also a significant increase in the crystallite size. The increase in the separation of the two intense crystalline peaks (α_1 and α_2), in analogy with other polyamides,[11] corresponds to an increase in the crystalline order (density). Note that the position of the peak at $2\theta = 20°$, which we associate with the H-bonded chains, does not change. This feature is also typical of polyamides.[11] These changes in the WAXD pattern suggest that addition of DMF leads to growth and perfection of the crystalline regions in PEA.

A DSC scan of a DMF-swollen film of 3–8 PEA (43 wt % DMF; 3 mg of DMF picked up by a 4-mg film) is shown in Figure 6 along with a similar scan of the dry 3–8 polymer. The differences in the two scans, for instance the exotherm at 83 °C in the DMF-swollen film, suggest that the structures of PEA in as-polymerized and DMF-swollen films are different. This is supported by the XRD and NMR data described below.

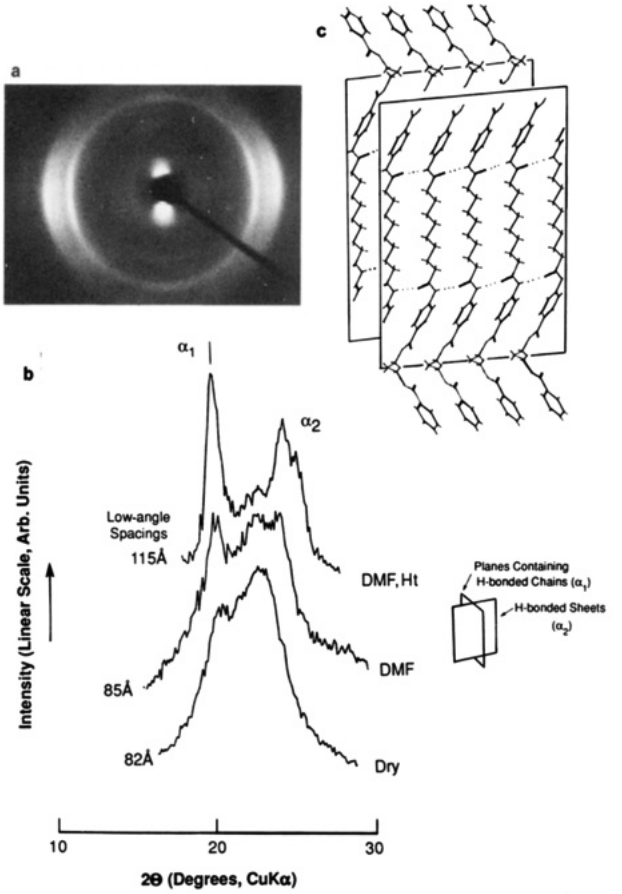

Figure 5. (a) Photograph of a DMF-treated 3–8 PEA. (b) WAXD scans of some of the samples used in Figure 4. (c) Model to illustrate the assignment of the two intense reflections to interference between H-bonded chains and H-bonded sheets.

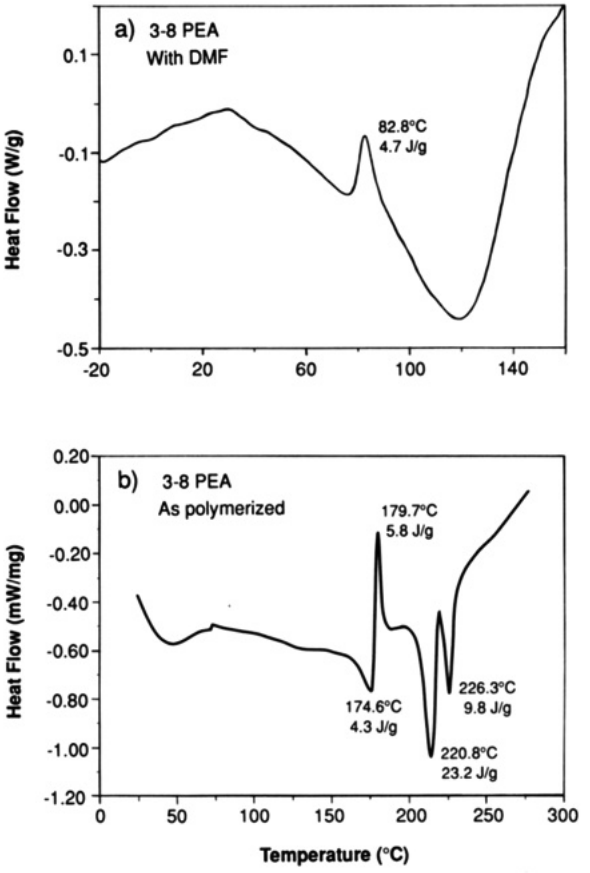

Figure 6. DSC scan of the 3–8 sample: (a) swollen in DMF; (b) as polymerized.

The NMR spectra and corresponding XRD scans of the 3–8 PEA before and after soaking in DMF (33 wt % DMF as calculated from the increase in the weight of the sample from 0.24 to 0.36 g) are shown in Figures 7 and 8, respectively. Also shown in the figures are the NMR and XRD data from as-polymerized crystalline powder. The assignments of the various NMR peaks are given in Figure 7 and are discussed in an earlier paper.[9] The four groups of peaks are assigned to the ester and amide carbons, the aromatic carbons, and the methylenes in the amide and the ester segments. Both the XRD and NMR data show that DMF induces crystallization in 3–8 PEA. The changes in the NMR peaks between 23 and 50 ppm show that crystallization is accompanied by large changes in the conformation of the interior methylene, in the methylene adjacent to the oxygen, and in the ester carbonyl. Preliminary BD/MAS spectra of dry and DMF-swollen PEA, also shown in Figure 7, are not significantly different from the CP/MAS spectra. The methylene chains exist in an all-trans conformation in both the crystalline and the amorphous state. Further, the local conformations of PEAs in the ordered and the disordered regions are similar.

Discussion

PEAs are thermotrophic liquid-crystalline (LC) polymers in which the LC behavior is due to the presence of interchain hydrogen bonds (H bonds) in the melt. We will focus here on the structure and the LC behavior of these polymers. The IR data from PEA in the solid state (Aharoni, S. M.; O'Brien, K., unpublished) show no evidence for any non-H-bonded amide groups. The "melting" temperature of these H-bonded chains is higher than that of the crystal lattice, the latter being the main melting event. Thus, at temperatures just above the melting point of the three-dimensional lattices, the H bonds are sufficiently strong even in the melt to sustain clusters of ordered molecules. These ordered clusters of H-bonded molecules are responsible for the LC behavior in these PEAs. The melting or the dissociation of the H-bonded sheets leads to an isotropic phase. Our XRD data show that the interchain H bonds do not always impose crystalline order in the solid phase in the equatorial plane but induce the amide groups to be in register along the fiber axis. As a consequence, the specimens quenched from the LC state in the molten polymer show LC features in the solid state.[12] This phase will be called the quenched liquid-crystalline (QLC) phase. We will discuss below the structural features of the crystalline, QLC, and LC phases.

The structure: The presence of only a diffuse halo along the equator and a series of sharp diffraction peaks along the meridian in the wide-angle fiber-diffraction patterns of oriented (hot-drawn) films of 3–4, 3–7, and 3–8 polymers (e.g., Figure 1) shows that the PEAs have liquidlike disorder in the equatorial plane and a high degree of crystalline or long-range order along the chain axis. These features are reminiscent of the smectic ordering found in liquid crystals. The WAXD photograph of the 3–8 film after exposure to DMF (Figure 5) shows that while the reflection due to the H-bonded sheets is along the equator, the reflection due to planes of H-bonded chains is ~7.5° off the equator. It is known from work on polyamides that, as indicated in Figure 5, the peaks at $2\theta \approx 20°$ and 23° are related to the distances between the H-bonded chains and sheets of these H-bonded chains, respectively.[13] Thus, the amide segments are nearly parallel to the fiber axis. We have noted in our publications[5] (Table V) that the fiber-axis repeat is shorter

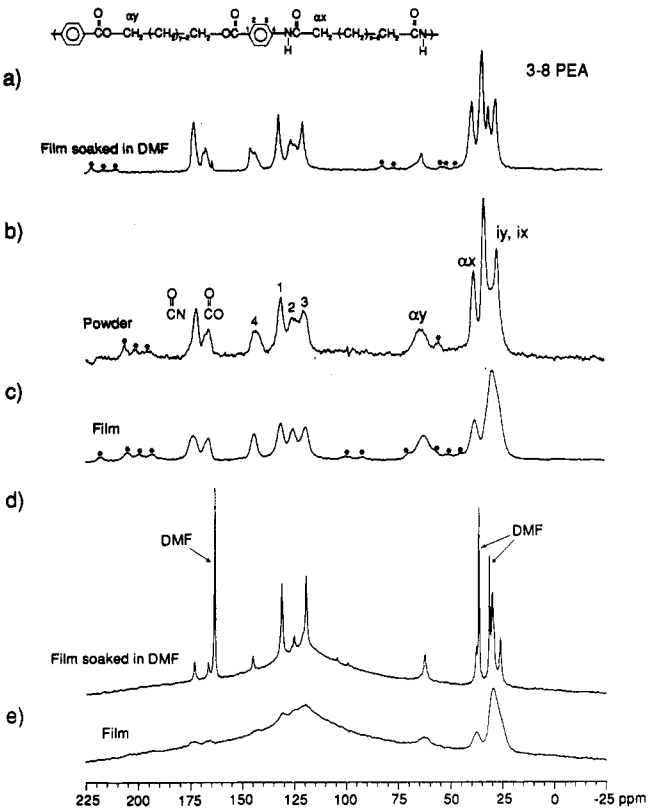

Figure 7. NMR spectra of 3–8 PEA. Scans a–c are CP/MAS spectra of the PEA in DMF, of an as-polymerized powder, and of a quenched film, respectively. Scans d and e are the BD/MAS spectra of the film after and before exposure to DMF, respectively. Peaks due to spinning sidebands are labeled with asterisks and should be ignored.

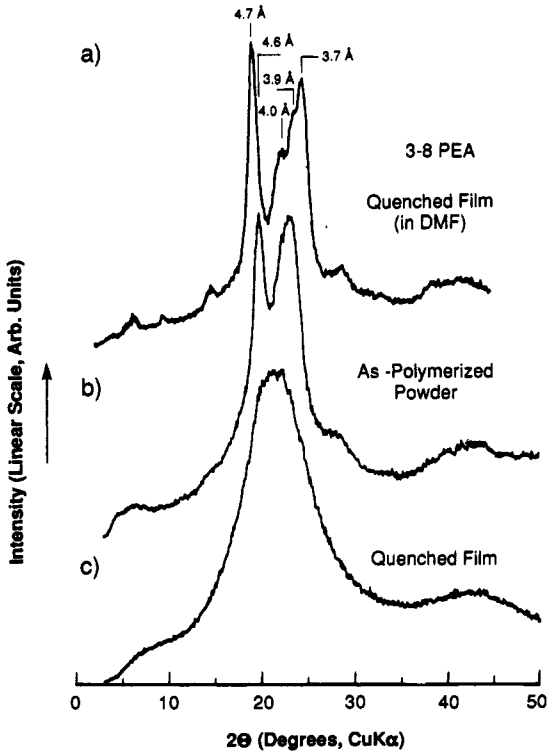

Figure 8. XRD scans of 3–8 PEA corresponding to the NMR scans in Figure 7a–c.

than the length of the monomer unit. In light of the fiber-axis orientation of the amide segments shown by the XRD photograph in Figure 5, the fiber-axis repeat could be shorter than the chemical length of the polymer only if

Table V
Analysis of X-ray Diffraction Patterns of Poly(ester amides)

polymer		calcd chain-axis length of the monomer, Å	obsd fiber-axis repeat, Å	obsd increment along fiber axis per $-CH_2-$, Å
y	*x*			
3	1	22.9	18.5	
				1.4
3	3	25.4	21.3	
				1.3
3	4	26.7	22.6	
				1.3
3	7	30.5	26.4	
				1.4
3	8	31.8	27.8	
				1.3
3	11	35.6	31.7	
				1.1
3	14	39.4	35.0	
5	11	38.1	32.0	
				1.2
5	14	41.9	35.6	
9	3	33.0	29.8	
				1.2
9	4	34.3	31.0	
				0.8
9	7	38.1	33.3	
				1.0
9	8	39.4	34.3	
				1.1
9	11	43.2	37.5	
				1.1
9	12	44.5	38.6	
				1.2
9	14	47.0	41.0	
2	14	38.1	34.6	
				0.4
3	14	39.4	35.0	
				0.2
4	14	40.6	35.2	
				0.4
5	14	41.9	35.6	
				1.4
9	14	47.0	41.0	
2	7	29.2	26.3	
				0.1
3	7	30.5	26.4	
				0.2
4	7	31.8	26.6	

the ester segments make a large angle with the fiber axis, as shown in Figure 5 for the 3–8 polymer. This is borne out by the data in Table V.[8] For each CH_2 unit added to the amide segments, the fiber-axis repeat increases by 1.3 Å, equal to the chemical length of the trans CH_2. For each CH_2 unit added to the ester segments, the fiber-axis repeat increases by ~0.4 Å. This can be attributed to an ~76° angle between the ester segments and the chain-axis direction as a result of the gauche conformation in the ester segments. This model (Figure 5) is consistent with the solid-state NMR data[8] but differs from our earlier model[5,8] in which an average tilt angle of 36° for the monomer as a whole was proposed.

Although DMF increases crystallinity and the degree of lateral order between the chains in the crystalline regions of the polymer, it is unlikely that DMF diffuses into the crystalline regions. These changes could be explained by the interactions of DMF with the amide groups in the amorphous regions of the polymer.[14] The NMR spectra of an as-polymerized powder and a DMF-swollen film are similar, but both of these are different from that of a film quenched from the melt. Thus, the conformations of the polymer chains in the LC phase (obtained, for example, by quenching the polymer from the melt) and the crystalline phases of the polymer (observed, for instance, in the as-polymerized and the DMF-swollen LC specimens)

are different. Preliminary evidence suggests that, as a result of these conformational differences, the chain-axis repeat in the semicrystalline phase is slightly lower than that in the QLC phase.

The long spacing (L) varies from ~67 to 180 Å depending on the history of the sample (Tables I–IV). Our results suggest that the conformational changes which bring about an increase in L occur in the melt or when chains are made mobile by the use of a plasticizer or by annealing (aging). On the basis of the accuracy with which we can define the peak maximum, we estimate the maximum error in long-spacing measurement at 85, 115, 140, 170, and 200 Å to be 2.5, 5, 7, 9, and 16 Å, respectively. The actual standard deviations calculated from several independent measurements are equal to or less than these values. The value of L appears to increase in increments of the length of the molecular repeat along the fiber axis. As shown in Tables I–IV, the fiber-axis repeat calculated assuming incremental increases in L ($L > 50$ Å) and constant fiber-axis repeat are in good agreement with the values calculated from wide-angle data.

The SAXS peak is essentially due to periodic fluctuations in the electron density along the fiber axis. Such fluctuations in semicrystalline polymers are commonly attributed to the presence of folded-chain lamellae. However, unlike in polymers with folded-chain lamellae, the increase in the SAXS peak intensity in PEA is not necessarily accompanied by increases in the lamellar repeat. Furthermore, an increase in the small-angle repeat by the re-formation of the folds will not give rise to a stepwise increase in L in polycrystalline, poorly crystallized specimens. Therefore, it is unlikely that folded-chain lamellae are present in PEA. While selective diffusion of DMF into the less ordered regions could account for the increase in the observed intensity of the SAXS peak, it cannot explain the observed stepwise increases of the long spacing. The exotherm seen in the DSC scan of the DMF-swollen sample (Figure 6) suggests that the increase in the crystalline order during the heating could be due to a crystalline phase transition. These changes in the crystalline regions are accompanied by an increase in the long spacing, for instance from 84 to 115 Å, and an increase in the SAXS peak intensity. Such changes are caused by both an increase in the molecular order within the crystalline layers and an increase in the disorder between the crystalline layers. We postulate that the changes in the packing of the rigid crystalline stems (hydrogen-bonded sheets) require changes in the conformation of the ester groups and speculate that these changes occur in increments so as to increase or decrease the long spacing by one chain repeat.

Our speculative model for the structure of PEA (Figure 9) is somewhat analogous to fringed-micelle model. The PEA chains form hydrogen-bonded sheets, and these sheets are stacked into layers as shown in Figure 5. These layers, under certain conditions, become organized into lamellae. The term lamellae is used here to indicate the crystallites of H-bonded, extended-chain segments. The conformations of the ester segments in all the chains within a lamella have to be the same for the lamellae to be crystalline. In the disordered interlamellar regions, multiple conformations of the ester segments could result in random orientation of the H bonds around the chain axis. The resulting electron density contrast can give rise to the SAXS peak. The SAXS peak with $L > 50$ Å and the broader peaks at repeat periods <50 Å are due to distances between the lamellae and the layers within the lamellae, respectively. The increments in L are almost equal to the

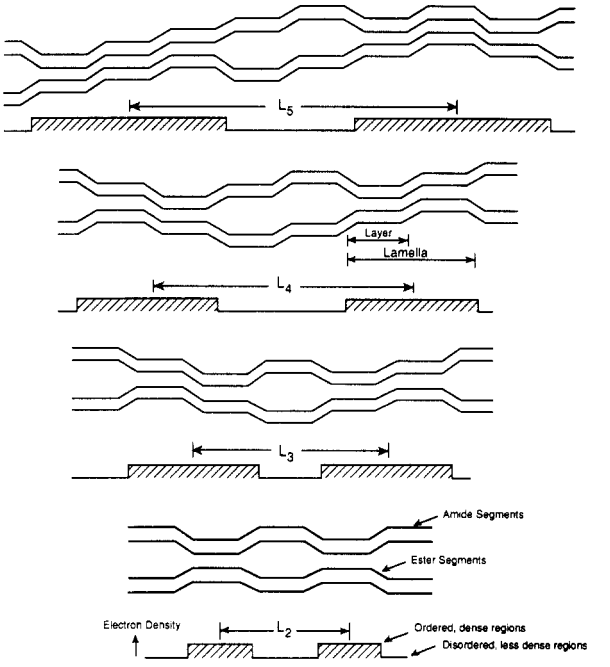

Figure 9. Model of lamellae consisting of hydrogen-bonded layers to explain our data.

layer repeat in the QLC phase, and these increments are not necessarily accompanied by changes in the structure within the lamellae. Thus, the changes in L could be due to the changes in the number of H-bonded layers in the disordered regions between the lamellae. Finally, the diffuse SAXS peak in the QLC phase and the sharpness of this peak in the semicrystalline phase suggest that the correlation between the lamellae in the QLC phase is poor and that the lamellae are well organized in the semicrystalline phase.

Liquid-crystalline behavior: In general, liquid-crystalline behavior is a result of the polymer chains behaving as rigid rods. In our case, because of the multiplicity of conformations possible in the ester segments, the chains are too flexible to produce LC behavior. In fact, the observed interdependency of the solution viscosity, the weight-average molecular weight, and the hydrodynamic radius[5] of PEAs with $y = 3$ and $x = 1$–12 is that expected of a flexible-chain, random-coil polymer. Hence, the single-chain properties are not responsible for the observed LC behavior.

Our data are consistent with the presence of lamellar crystalline regions separated by amorphous domains. The thickness of these lamellae corresponds to more than one chain-axis repeat or more than one layer of H-bonded sheets (Figure 9). The LC behavior of the polymer is due to the persistence of H-bonded layers and correlations between these layers (i.e., lamellar structures) in the melt. The observation of long spacings larger than the chain-axis repeat indicates the presence of various types of smectic structures and interlamellar correlations. The increase in the long spacing in what appears to be integral steps of this repeat suggests that the degree of these correlations decreases in discrete steps as the three-dimensional arrangement of the H-bonded sheets disappears at temperatures between the melting point and the isotropization temperature of the polymer. This stepwise melting of the various smectic structures might explain the small melting peaks present in the DSC scans past the main melting endotherm. In fact, the number of peaks in the DSC scan decreases if the sample is reheated after cooling from above the melting temperature and below the isotro-

pization temperature. An isotropic phase is obtained when the H bonds within the layers are too weak or when the fraction of the H-bonded chains is too small to sustain anisotropic H-bonded layers. Thus, the rigidity of the H-bonded sheets, the anisotropy of the lamellae composed of layers of H-bonded sheets, and the correlation between the lamellae are the reasons for the observed LC behavior in these PEAs. In other words, birefringence in the melt is due to the presence of H-bonded sheets in the form of clusters, layers, or lamellae.

We speculate that the changes in the conformation of the ester segment and the lamellar repeat are interrelated, and the various postmelting structures are the result of regularly spaced conformational barriers in the ester moiety. In fact, solid-state NMR results show that while the amide regions of the polymer are exclusively in the trans conformation, a mixture of trans and gauche (sometimes exclusively gauche) conformations is present in the ester moiety.[8,9] Such a site-specific conformational change of the chain might explain the stepwise increase in the lamellar spacing. LC behavior is observed in PEAs only when the ester and the amide segments are strictly alternating, as in the polymers studied here. LC behavior is not observed when the placement of the amide and the ester segments is random[15-17] or when only amides[18] or esters[19] are present along the main chain. These results show that the presence of rigid H-bonded sheets separated by ester groups with multiple conformations, which therefore function as flexible spacers, is essential to the formation of a LC phase in PEAs.

Acknowledgment. We thank Dr. G. R. Hatfield for obtaining the NMR scans, Dr. W. B. Hammond for providing the diagram of the H-bonded sheets from which the model shown in Figure 5 was prepared, and Prof. S. Krimm for extensive discussions.

References and Notes

(1) Flory, P. J. *Adv. Polym. Sci.* **1984**, *59*, 1.
(2) Murthy, N. S. *Biopolymers* **1984**, *23*, 1261.
(3) Folda, T.; Hoffmann, H.; Chanzy, H.; Smith, P. *Nature* **1988**, *333*, 55.
(4) Jeffrey, G. A. *Acc. Chem. Res.* **1986**, *19*, 168.
(5) Aharoni, S. M. *Macromolecules* **1988**, *21*, 1941.
(6) Aharoni, S. M. *Macromolecules* **1989**, *22*, 686.
(7) Aharoni, S. M. *Macromolecules* **1989**, *22*, 1125.
(8) Aharoni, S. M.; Correale, S. T.; Hammond, W. B.; Hatfield, G. R.; Murthy, N. S. *Macromolecules* **1989**, *22*, 1137.
(9) Hatfield, G. R.; Aharoni, S. M. *Macromolecules* **1989**, *22*, 3807.
(10) Murthy, N. S. *Norelco Rep.* **1983**, *30*, 35.
(11) Murthy, N. S.; Minor, H.; Latif, R. A. *J. Macromol. Sci., Phys.* **1987**, *B26*, 427.
(12) Thomas, E. L.; Wood, B. A. *Faraday Discuss. Chem. Soc.* **1985**, *79*, 229.
(13) Murthy, N. S.; Curran, S. A.; Aharoni, S. M. *Macromolecules* **1991**, *24*, 3215.
(14) Murthy, N. S.; Stamm, M.; Sibilia, J. P.; Krimm, S. *Macromolecules* **1989**, *22*, 1261.
(15) He, Z.; Whitcombe, M. J.; Mitchell, G. R. *Br. Polym. J.* **1990**, *23*, 41.
(16) Laakso, T. M.; Reynolds, D. D. *J. Am. Chem. Soc.* **1960**, *82*, 3640.
(17) Manzini, G.; Crescenti, V.; Ciana, A.; Ciceri, L.; Della Fortuna, G.; Zotteri, L. *Eur. Polym. J.* **1973**, *9*, 941.
(18) Shashoua, V. E.; Eareckson, W. M. *J. Polym. Sci.* **1959**, *40*, 343.
(19) Farrow, G.; McIntosh, J.; Ward, I. M. *Makromol. Chem.* **1960**, *82*, 3640.